Electron spectrum and superconductivity in the *t-J* model at moderate doping

N. M. Plakida
Max-Planck-Institut für Physik Komplexer Systeme, Nöthnitzerstrasse 38, D-01187 Dresden, Germany
and Joint Institute for Nuclear Research, 141980 Dubna, Russia

V. S. Oudovenko
Joint Institute for Nuclear Research, 141980 Dubna, Russia
and Max-Planck-Institut für Festkörperforschung, Heisenbergstrasse 1, D-70569 Stuttgart, Germany
(Received 8 July 1998)

A microscopical theory of electron spectrum and superconductivity within the two-dimensional *t-J* model in paramagnetic state is proposed. By employing the projection technique for the Green functions in terms of the Hubbard operators self-consistent Eliashberg equations are derived. A strong coupling of electrons with spin and charge fluctuations due to exchange and kinematical interactions is obtained. In the normal state, one-electron spectral functions reveal narrow quasiparticle peaks close to the Fermi surface (FS) with an additional broad incoherent band. The FS changes from holelike at low doping to electronlike for hole concentrations $\delta > 0.3$. In the superconducting state we observe *d*-wave pairing with the maximal $T_c \simeq 0.04t$ at optimal doping $\delta \simeq 0.3$. [S0163-1829(99)04513-0]

I. INTRODUCTION

Experimental studies of high-temperature superconductors have provided strong support for a major role of strong electron correlations in copper-oxide materials as was first proposed by Anderson.[1,2] Among them are recent studies of electronic spectra by angle-resolved photoemission spectroscopy (ARPES) which reveal a quite unusual behavior for the Fermi liquid in the normal state (for a review, see Ref. 3). A very broad quasiparticle peaks with a pseudogap formation of the *d*-wave-like symmetry at the Fermi surface[4,5] or even the Fermi surface destruction in underdoped regime have been reported.[6] Direct measurements of the superconducting gap and the normal state pseudogap by the technique of tunnelling spectroscopy (see, e.g., Refs. 7 and 8, and references therein) suggest that both gaps have the same microscopical origin.

One of the possible scenarios of the gap formation is a strong coupling of doped holes to antiferromagnetic (AFM) spin fluctuations (see, e.g., Ref. 9). The problem can be studied within the simplest *t-J* model[1,10] which is believed to take properly into account spin correlations and hole kinematics. In the limit of small hole concentrations one can consider a one-hole motion on the AFM background within the spin-polaron representation for the *t-J* model.[11,12] A number of studies of the model (see, e.g., Refs. 13–16, and references therein) predicted that a doped hole dressed by AFM spin fluctuations can propagate coherently as a spin-polaron quasiparticle (QP) which was proved later in ARPES experiments.[17] It was also suggested that the same spin fluctuations could mediate a superconducting pairing of the spin-polaron QP. The problem was treated within the BCS formalism for phenomenological models of pairing interaction in Refs. 18 and 19. A self-consistent numerical solution of the strong coupling Eliashberg equations for spin-polarons and magnons has been given in Ref. 20. A strong renormalization of the hole spectrum due to spin fluctuations and the *d*-wave pairing of spin polaron QP with maximal $T_c \simeq 0.01t$ were obtained at optimal hole concentration $\delta \simeq 0.2$. In Ref. 21 the superconducting instability within the spin-polaron model was obtained only with additional electron-phonon coupling.

At moderate doping only short-range dynamical AFM correlations exist and the spin-polaron model becomes inadequate. To deal with the strong coupling limit for the Hubbard model and the *t-J* model a number of numerical methods for finite clusters has been developed (for review, see Ref. 22). Spectral properties in the normal state of the two-dimensional *t-J* model at moderate doping have been investigated by exact diagonalization[23] which show a large electronic Fermi surface and a quasiparticlelike spectrum with large incoherent background. Spectral functions of the *t-J* model were considered also by using the finite-temperature Lanczos method.[24] A large asymmetry between the hole and electron spectra was observed with a strong damping for the hole spectra.

Concerning the superconducting pairing in the *t-J* model formation of the $d_{x^2-y^2}$ pairing correlations due to strong AFM spin fluctuations were observed for small clusters. However, as has been recently shown by applying the constrained-path Monte Carlo method[25] to the two-dimensional Hubbard model the $d_{x^2-y^2}$ pairing correlations vanish with increasing lattice size or the Coulomb repulsion. By using the power-Lanczos method, it has been concluded (see Ref. 26) that the two-dimensional *t-J* model does not have long-range *d*-wave superconducting correlations for $J/t \leqslant 0.5$. In spite of important information obtained via numerical techniques, the finite cluster calculations due to known limitations (finite size effects, few filling fractions, etc.) can give only restricted information concerning the low-energy spectral properties and gap formation. So to study the spectral properties and possible superconducting pairing in the strong coupling limit an analytical treatment is highly demanded.

The main problem in analytical studies of the t-J model is the so-called kinematical interaction imposed by the projected character of electron operators acting in the subspace of singly occupied lattice sites.[27] To take into account the constraints of no double occupancy different types of slave-boson (-fermion) techniques were proposed (see Refs. 28–31, and references therein). In the mean field approximation (MFA) the local constraints are approximated by a global one, that reduces the problem to free fermions and bosons in the mean field.[28] To treat the constraints in a systematic way, in Refs. 29 and 30 a large-N expansion, with N being the number of states (orbitals) at a lattice cite, was used. In that approach the local constraints are relaxed and a weak coupling approximation is possible. By using the $1/N$ expansion, the d-wave superconducting instability induced by the exchange interaction was obtained in the t-J model close to half filling.[30] The Baym-Kadanoff variational technique for the Green functions in terms of the Hubbard operators was used in Refs. 32 and 33 (also in the limit of large N) to consider superconducting pairing in the t-J model. For a finite J the d-wave superconducting instability mediated by exchange and charge fluctuations was obtained below $T_c \simeq 0.01t$. However, in the large-N expansion the kinematical interaction is suppressed and this approach, being rigorous in the limit $N\rightarrow\infty$, is difficult to extrapolate to real spin systems with $N=2$.

A formally rigorous method to treat the unconventional commutation relations for the projected electron operators is based on the diagram technique for the Hubbard operators,[34,35] since in this method the local constraints are rigorously implemented by the Hubbard operator algebra. A superconducting pairing due to the kinematical interaction in the Hubbard model in the limit of strong electron correlations ($U\rightarrow\infty$) was first obtained by Zaitsev and Ivanov[36] who studied the lowest order diagrams for a two-particle vertex equation. Their approximation, being equivalent to the MFA for a superconducting order parameter, gives only the s-wave pairing. As was shown later,[37,38] the s-wave pairing in the limit of strong correlations violates an exact requirement of no single-site pairs and should be rejected. By applying the MFA for the Green functions in terms of the Hubbard operators it was proved in Refs. 37 and 38 that the d-wave superconducting pairing mediated by the exchange interaction is thermodynamically stable and has high $T_c \simeq 0.1t$ for $J=0.4t$.

On the basis of the diagram technique, detailed studies of spin fluctuations and superconducting pairing in the t-J model were performed by Izyumov *et al.*[39] Summation of the first order diagrams for the self-energy reproduced the results of the MFA in Refs. 37 and 38. Estimations done in the weak coupling limit for the Eliashberg equation with account of the second order diagrams revealed quite a low superconducting T_c.

To study the scenario of Cooper pair formation at high temperature in the present paper we consider a theory of electron spectrum and superconducting pairing for the t-J model in paramagnetic state by applying the projection technique[40] for the Green functions[41] in terms of the Hubbard operators. To go beyond of the MFA in Refs. 37 and 38 we derived the Eliashberg equations in the noncrossing approximation and numerically solve it. As is usual in the Eliashberg theory, we fix the phase of the gap function by taking it to be real that excludes phase fluctuations and gives a finite T_c for the gap formation in two dimensions. At high temperature $T>T_c$ we observe narrow QP peaks for single-electron spectral functions near FS and a broad incoherent band below FS. The latter results in nonzero occupation numbers $n_{\mathbf{k},\sigma}$ throughout the Brillouin zone which show only a small drop, increasing with doping, at FS. A direct numerical solution of the linearized gap equation reveals the d-wave superconducting instability with maximal $T_c \simeq 0.04t$ at optimal doping $\delta \simeq 0.3$.

The paper is organized as follows. In the next section we present the Dyson equation for the matrix Green function in terms of the Hubbard operators. In Sec. III self-consistent Eliashberg equations in the noncrossing approximation are derived. In Sec. IV numerical results for the single-electron spectral functions, occupation numbers $n_{\mathbf{k},\sigma}$, a superconducting gap function, and T_c are presented and discussed. Conclusions are given in Sec. V.

II. DYSON EQUATION FOR THE t-J MODEL

We consider the t-J model in the standard notation[1,10]

$$H_{t-J}=-t\sum_{i\neq j,\sigma}\tilde{a}^{+}_{i\sigma}\tilde{a}_{j\sigma}+J\sum_{\langle ij\rangle}\left(\mathbf{S}_i\mathbf{S}_j-\frac{1}{4}n_in_j\right), \tag{1}$$

where $\tilde{a}^{+}_{i\sigma}=a^{+}_{i\sigma}(1-n_{i-\sigma})$ are projected electron operators and $S^{\alpha}_i=(1/2)\Sigma_{s,s'}\tilde{a}^{+}_{is}\sigma^{\alpha}_{s,s'}\tilde{a}_{is'}$ are spin-1/2 operators. Here t is an effective transfer integral and J is the antiferromagnetic exchange energy for a pair of nearest neighbor sites $\langle ij\rangle$, $i>j$.

To take into account on a rigorous basis the projected character of electron operators we employ the Hubbard operator (HO) technique.[42] The HO's are defined as

$$X^{\alpha\beta}_i=|i,\alpha\rangle\langle i,\beta| \tag{2}$$

for three possible states at a lattice site i: $|i,\alpha\rangle=|i,0\rangle$, $|i,\sigma\rangle$ for an empty site, and for a singly occupied site by an electron with spin $\sigma/2$ ($\sigma=\pm1$, $\bar{\sigma}=-\sigma$). They obey the completeness relation

$$X^{00}_i+\sum_{\sigma}X^{\sigma\sigma}_i=1, \tag{3}$$

which rigorously preserves the constraint of no double occupancy.

By using the Hubbard operator representation (2) for $\tilde{a}^{+}_{i\sigma}=X^{\sigma 0}_i$ and $\tilde{a}_{j\sigma}=X^{0\sigma}_j$ and for spin and number operators we write the Hamiltonian of the t-J model (1) in a more general form:

$$H_{t-J}=-\sum_{i\neq j,\sigma}t_{ij}X^{\sigma 0}_iX^{0\sigma}_j-\mu\sum_{i\sigma}X^{\sigma\sigma}_i$$
$$+\frac{1}{4}\sum_{i\neq j,\sigma}J_{ij}(X^{\sigma\bar{\sigma}}_iX^{\bar{\sigma}\sigma}_j-X^{\sigma\sigma}_iX^{\bar{\sigma}\bar{\sigma}}_j). \tag{4}$$

Here we introduced the electron hopping energy for the nearest neighbors, $t_{ij}=t$, and the second neighbors, $t_{ij}=t'$, on a 2D square lattice, and the exchange interaction $J_{ij}=J$ for the

nearest neighbors. These parameters can be considered as independent ones if starting from a more realistic for copper oxides three-band p-d model we reduce it to the t-J model[10] (see Ref. 43). The chemical potential μ is to be calculated from the equation for the average number of electrons

$$n=\sum_{\sigma}\langle X_i^{\sigma\sigma}\rangle. \tag{5}$$

To discuss the superconducting pairing within the model (4) we consider the matrix Green function (GF)

$$\hat{G}_{ij,\sigma}(t-t')=\langle\langle\Psi_{i\sigma}(t)|\Psi_{j\sigma}^{+}(t')\rangle\rangle \tag{6}$$

in terms of the Nambu operators

$$\Psi_{i\sigma}=\begin{pmatrix}X_i^{0\sigma}\\ X_i^{\bar{\sigma}0}\end{pmatrix},\quad \Psi_{i\sigma}^{+}=(X_i^{\sigma 0}\ \ X_i^{0\bar{\sigma}}), \tag{7}$$

where Zubarev's notation for the anticommutator Green function (6) is used.[41]

By differentiating the GF (6) over the time t we get the following equation:

$$\omega\hat{G}_{ij\sigma}(\omega)=\delta_{ij}\hat{Q}_{\sigma}+\langle\langle\hat{Z}_{i\sigma}|\Psi_{j\sigma}\rangle\rangle_{\omega}, \tag{8}$$

where $\hat{Z}_{i\sigma}=[\Psi_{i\sigma},H]$, $\hat{Q}_{\sigma}=\left(\begin{smallmatrix}Q_{\sigma} & 0\\ 0 & Q_{\bar{\sigma}}\end{smallmatrix}\right)$ with $Q_{\sigma}=\langle X_i^{00}+X_i^{\sigma\sigma}\rangle$. Since we consider a spin-singlet state the correlation function $Q_{\sigma}=Q=1-n/2$ depends only on the average number of electrons (5).

Now, we project the many-particle GF in Eq. (8) on the single-electron GF by introducing the *irreducible* part of $\hat{Z}_{i\sigma}$ operator

$$\langle\langle\hat{Z}_{i\sigma}|\Psi_{j\sigma}^{+}\rangle\rangle=\sum_{l}\hat{E}_{il\sigma}\langle\langle\Psi_{l\sigma}|\Psi_{j\sigma}^{+}\rangle\rangle+\langle\langle\hat{Z}_{i\sigma}^{(\mathrm{irr})}|\Psi_{j\sigma}^{+}\rangle\rangle,$$

$$\langle\{\hat{Z}_{i\sigma}^{(\mathrm{irr})},\Psi_{j\sigma}^{+}\}\rangle=\langle\hat{Z}_{i\sigma}^{(\mathrm{irr})}\Psi_{j\sigma}^{+}+\Psi_{j\sigma}^{+}\hat{Z}_{i\sigma}^{(\mathrm{irr})}\rangle=0, \tag{9}$$

that results in the equation for the frequency matrix

$$\hat{E}_{ij\sigma}=\langle\{[\Psi_{i\sigma},H],\Psi_{j\sigma}^{+}\}\rangle Q^{-1}. \tag{10}$$

To calculate the matrix (10) we use the equation of motion for the HO

$$\left(i\frac{d}{dt}+\mu\right)X_i^{0\sigma}=-\sum_{l}t_{il}B_{i\sigma\sigma'}X_l^{0\sigma'}+\frac{1}{2}\sum_{l}J_{il}(B_{l\sigma\sigma'}-\delta_{\sigma\sigma'})X_i^{0\sigma'}, \tag{11}$$

where we introduced the operator

$$B_{i\sigma\sigma'}=(X_i^{00}+X_i^{\sigma\sigma})\delta_{\sigma'\sigma}+X_i^{\bar{\sigma}\sigma}\delta_{\sigma'\bar{\sigma}}=\left(1-\frac{1}{2}N_i+\sigma S_i^{z}\right)\delta_{\sigma'\sigma}+S_i^{\bar{\sigma}}\delta_{\sigma'\bar{\sigma}}. \tag{12}$$

The Bose-like operator (12) describes electron scattering on spin and charge fluctuations caused by the nonfermionic commutation relations for the HO [the first term in Eq. (11)—the kinematical interaction] and by the exchange spin-spin interaction [the second term in Eq. (11)].

The frequency matrix (10) defines the zero-order GF in the generalized MFA

$$\hat{G}_{ij\sigma}^{0}(\omega)=Q\{\omega\hat{\tau}_0\delta_{ij}-\hat{E}_{ij\sigma}\}^{-1}. \tag{13}$$

By writing the equation of motion for the irreducible part of the GF in Eq. (9) with respect to the second time t' for the right-hand side operator $\Psi_{j\sigma}^{+}(t')$ and performing the same projection procedure as in Eq. (9) we can obtain the Dyson equation for the GF (6) in the form

$$\hat{G}_{ij\sigma}(\omega)=\hat{G}_{ij\sigma}^{0}(\omega)+\sum_{kl}\hat{G}_{ik\sigma}^{0}(\omega)\hat{\Sigma}_{kl\sigma}(\omega)\hat{G}_{lj\sigma}(\omega), \tag{14}$$

where the self-energy operator $\hat{\Sigma}_{kl\sigma}(\omega)$ is defined by the equation

$$\hat{T}_{ij\sigma}(\omega)=\hat{\Sigma}_{ij\sigma}(\omega)+\sum_{kl}\hat{\Sigma}_{ik\sigma}(\omega)\hat{G}_{kl\sigma}^{0}(\omega)\hat{T}_{lj\sigma}(\omega). \tag{15}$$

Here the scattering matrix is given by

$$\hat{T}_{ij\sigma}(\omega)=Q^{-1}\langle\langle\hat{Z}_{i\sigma}^{(\mathrm{irr})}|\hat{Z}_{j\sigma}^{(\mathrm{irr})^{+}}\rangle\rangle_{\omega}Q^{-1}. \tag{16}$$

From Eq. (15) it follows that the self-energy operator is given by the *proper* part of the scattering matrix (16) that has no parts connected by the single zero-order GF (13):

$$\hat{\Sigma}_{ij\sigma}(\omega)=Q^{-1}\langle\langle\hat{Z}_{i\sigma}^{(\mathrm{irr})}|\hat{Z}_{j\sigma}^{(\mathrm{irr})^{+}}\rangle\rangle_{\omega}^{(\mathrm{prop})}Q^{-1}. \tag{17}$$

Equations (13), (14), and (17) give an exact representation for the single-electron GF (6). To calculate it, however, one has to introduce an approximation for the many-particle GF in the self-energy matrix (17) which describes inelastic scattering of electrons on spin and charge fluctuations.

III. SELF-CONSISTENT ELIASHBERG EQUATIONS

In the **k** representation for the GF

$$G_{\sigma}^{\alpha\beta}(k,\omega)=\sum_{j}G_{oj\sigma}^{\alpha\beta}(\omega)e^{-i\mathbf{kj}}, \tag{18}$$

we get for the zero-order GF (13)

$$\hat{G}_{\sigma}^{(0)}(k,\omega)^{-1}=\{\omega\hat{\tau}_0-(E_k^{\sigma}-\tilde{\mu})\hat{\tau}_3-\Delta_k^{\sigma}\hat{\tau}_1\}Q^{-1}, \tag{19}$$

where $\hat{\tau}_0,\hat{\tau}_1,\hat{\tau}_3$ are the Pauli matrices. The energy of the quasiparticles E_k^{σ}, the renormalized chemical potential $\tilde{\mu}=\mu-\delta\mu$ and the gap function Δ_k^{σ} in the MFA (10) are given by

$$E_k^{\sigma}=-\epsilon(k)Q-\epsilon_s(k)/Q-\frac{2J}{N}\sum_{q}\gamma(k-q)N_{q\sigma}, \tag{20}$$

where we have introduced $J(q)=4J\gamma(q)$ and $\epsilon(k)=t(k)=4t\gamma(k)+4t'\gamma'(k)$, $\epsilon_s(k)=4t\gamma(k)\chi_{1s}+4t'\gamma'(k)\chi_{2s}$, with $\gamma(k)=(1/2)(\cos a_xq_x+\cos a_yq_y)$ and $\gamma'(k)=\cos a_xq_x\cos a_yq_y$,

$$\delta\mu=\frac{1}{N}\sum_{q}\epsilon(q)N_{q\sigma}-2J\left(\frac{n}{2}-\frac{\chi_{1s}}{Q}\right), \tag{21}$$

$$\Delta_k^\sigma = -\frac{2}{NQ}\sum_q g(q,k-q)\langle X_{-q}^{0\bar{\sigma}} X_q^{0\sigma}\rangle, \tag{22}$$

where the interaction is given by the function

$$g(q,k-q) = t(q) - \frac{1}{2}J(k-q). \tag{23}$$

There are two contributions in the gap equation (22): the **k**-independent kinematical interaction $t(q)$ and the exchange interaction $J(k-q)$. The kinematical interaction gives no contribution to the *d*-wave pairing in MFA, Eq. (22) (see Ref. 37), and we disregard it in the following equations. The average number of electrons in Eqs. (20) and (21) in the **k** representation is written in the form

$$n_{k,\sigma} = \langle X_k^{\sigma 0} X_k^{0\sigma}\rangle = QN_{k\sigma}. \tag{24}$$

In calculation of the normal part of the frequency matrix (20) we have neglected the charge fluctuations and introduced the spin correlation functions:

$$\chi_{1s} = \langle \mathbf{S}_i \mathbf{S}_{i+a_1}\rangle, \quad \chi_{2s} = \langle \mathbf{S}_i \mathbf{S}_{i+a_2}\rangle, \tag{25}$$

for the nearest χ_{1s} $[a_1 = (\pm a_x, \pm a_y)]$ and the next-nearest χ_{2s} $[a_2 = \pm(a_x \pm a_y)]$ neighbor lattice sites.

To calculate the self-energy operator we employ the noncrossing approximation (or the self-consistent Born approximation) for the *proper* part of the many-particle Green function in Eq. (17). It is given by the two-time decoupling for the corresponding correlation functions in Eq. (17)

$$\langle X_{j'}^{\sigma' 0} B_{j\sigma\sigma'}^+ X_{i'}^{0\sigma'}(t) B_{i\sigma\sigma'}(t)\rangle \simeq \langle X_{j'}^{\sigma' 0} X_{i'}^{0\sigma'}(t)\rangle \langle B_{j\sigma\sigma'}^+ B_{i\sigma\sigma'}(t)\rangle. \tag{26}$$

The proposed decoupling does not violate equal time correlations since in Eq. (26) $j \neq j'$ and $i \neq i'$. In the adopted approximation vertex corrections are neglected while the Fermi-like and the Bose-like correlation functions are supposed to be calculated self-consistently from the full Green functions. As was argued in Ref. 44 where the analogous approximation was used, at moderate doping we can consider the spin-charge fluctuations and single-particle excitations as independent modes. Then we can perform the decoupling (26) in the framework of the mode-coupling approximation which has been proved to be quite a reliable one even for systems with strong interactions. As was shown for the spin-polaron *t*-*J* model the vertex corrections to the noncrossing approximation are small and give only numerical renormalization of the model parameters (see, e.g., Ref. 14).

Using the spectral representation for the GF, we obtain in the noncrossing approximation the following expression for the normal and anomalous components of the self-energy:

$$\tilde{\Sigma}_{11(12)}^\sigma(k,\omega) = Q\hat{\Sigma}_{11(12)}^\sigma(k,\omega) = \frac{1}{N}\sum_q \int\int_{-\infty}^{+\infty} dz\, d\Omega\, N(\omega,z,\Omega) \times \lambda_{11(12)}(q,k-q|\Omega) A_{11(12)}^\sigma(q,z), \tag{27}$$

where

$$N(\omega,z,\Omega) = \frac{1}{2}\frac{\tanh(z/2T) + \coth(\Omega/2T)}{\omega - z - \Omega}. \tag{28}$$

Here we introduce the spectral density

$$A_{11}^\sigma(q,z) = -\frac{1}{Q\pi}\mathrm{Im}\langle\langle X_q^{0\sigma} | X_q^{\sigma 0}\rangle\rangle_{z+i\delta}, \tag{29}$$

$$A_{12}^\sigma(q,z) = -\frac{1}{Q\pi}\mathrm{Im}\,\langle\langle X_q^{0\sigma} | X_{-q}^{0\bar{\sigma}}\rangle\rangle_{z+i\delta}, \tag{30}$$

and the electron-electron interaction functions caused by spin-charge fluctuations

$$\lambda_{11(12)}(q,k-q|\Omega) = g^2(q,k-q) \times\left[-\frac{1}{\pi}\mathrm{Im}\, D^\pm(k-q,\Omega+i\delta)\right], \tag{31}$$

where the spectral density for the spin-charge fluctuations is defined by the bosonlike commutator GF

$$D^\pm(q,\Omega) = \langle\langle \mathbf{S}_q | \mathbf{S}_{-q}\rangle\rangle_\Omega \pm \frac{1}{4}\langle\langle n_q | n_q^+\rangle\rangle_\Omega. \tag{32}$$

The solution of the Dyson equation (14) can be written in the Eliashberg notation as

$$\hat{G}^\sigma(k,\omega) = Q\tilde{G}^\sigma(k,\omega) = Q\frac{\omega Z_k^\sigma(\omega)\hat{\tau}_0 + [E_k^\sigma + \xi_k^\sigma(\omega) - \tilde{\mu}]\hat{\tau}_3 + \Phi_k^\sigma(\omega)\hat{\tau}_1}{[\omega Z_k^\sigma(\omega)]^2 - [E_k^\sigma + \xi_k^\sigma(\omega) - \tilde{\mu}]^2 - |\Phi_k^\sigma(\omega)|^2}, \tag{33}$$

where

$$\omega[1 - Z_k^\sigma(\omega)] = \frac{1}{2}[\tilde{\Sigma}_{11}^\sigma(k,\omega) + \tilde{\Sigma}_{22}^\sigma(k,\omega)],$$

$$\xi_k^\sigma(\omega) = \frac{1}{2}[\tilde{\Sigma}_{11}^\sigma(k,\omega) - \tilde{\Sigma}_{22}^\sigma(k,\omega)], \tag{34}$$

$$\Phi_k^\sigma(\omega) = \Delta_k^\sigma + \tilde{\Sigma}_{12}^\sigma(k,\omega),$$

and $\Sigma_{11}^\sigma(k,\omega) = -\Sigma_{22}^{\bar{\sigma}}(-k,-\omega)$. Here we fix the phase of the gap function by taking it to be real.

IV. NUMERICAL RESULTS AND DISCUSSION

For numerical solution of the system of equations (27)–(34) we have used the imaginary frequency representation for the Green function (33) with $\omega = i\omega_n = i\pi T(2n+1)$ and the spin-charge Green function (32) with $\Omega = i\omega_n = i\pi T 2n$ where $n = 0, \pm 1, \pm 2, \ldots$. By using the representation for the function (28)

$$N(i\omega_n,z,\Omega) = -T\sum_m \frac{1}{i\omega_m - z}\frac{1}{i(\omega_n - \omega_m) - \Omega} \tag{35}$$

after integration in Eq. (27) we get

$$\tilde{\Sigma}^{\sigma}_{11(12)}(k,i\omega_n) = -\frac{T}{N}\sum_q \sum_m \tilde{G}^{\sigma}_{11(12)}(q,i\omega_m) \times \lambda_{11(12)}(q,k-q|i\omega_n - i\omega_m). \quad (36)$$

The interaction functions are given by

$$\lambda_{11(12)}(q,k-q|i\omega_\nu) = g^2(q,k-q)D^{\pm}(k-q,i\omega_\nu). \quad (37)$$

To calculate superconducting T_c it is sufficient to study a linearized system of the Eliashberg equations (34) which has the following form:

$$\tilde{G}^{\sigma}_{11}(k,i\omega_n) = \frac{1}{i\omega_n - E_k + \tilde{\mu} - \tilde{\Sigma}^{\sigma}_{11}(k,i\omega_n)}, \quad (38)$$

$$\Phi^{\sigma}(k,i\omega_n) = \Delta^{\sigma}_k + \phi^{\sigma}(k,i\omega_n) = \frac{T}{N}\sum_q \sum_m \{J(k-q) + \lambda_{12}(q,k-q|i\omega_n - i\omega_m)\} \times \tilde{G}^{\sigma}_{11}(q,i\omega_m)\tilde{G}^{\bar{\sigma}}_{11}(q,-i\omega_m)\Phi^{\sigma}(q,i\omega_m). \quad (39)$$

At first the system of equations for the normal GF (38) was solved numerically for a given concentration of electrons

$$\frac{n}{1-n/2} = \frac{1}{N}\sum_{k,\sigma} N_{k\sigma} = 1 + \frac{2T}{N}\sum_k \sum_{n=-\infty}^{\infty} \tilde{G}_{11}(k,i\omega_n). \quad (40)$$

Then the eigenvalues and eigenfunctions of the gap function (39) were calculated to obtain the superconducting transition temperature T_c and the $(\mathbf{k},\omega)$ dependence of the gap function.

For numerical calculations we take into account only the spin-fluctuation contribution and write the function $D^{\pm}_s(q,i\omega_\nu)$ (32) in the form

$$D^{\pm}_s(q,i\omega_\nu) \simeq \langle\langle \mathbf{S}_q | \mathbf{S}_{-q}\rangle\rangle_{i\omega_\nu} = -\int_0^{+\infty} \frac{2z\,dz}{z^2+\omega_\nu^2}\chi''_s(q,z). \quad (41)$$

To perform self-consistent calculations one should write an equation for the spin-fluctuation susceptibility (41) in terms of the one-electron Green function (38) as has been done, e.g., in Ref. 45. However, to make our numerical work tractable in the present paper we use a model reperesentation for the spin-fluctuation susceptibility suggested in numerical studies[46]

$$\chi''_s(q,\omega) = -\frac{1}{\pi}\mathrm{Im}\langle\langle \mathbf{S}_q | \mathbf{S}_{-q}\rangle\rangle_{\omega+i\delta} = \chi_s(q)\chi''_s(\omega) = \frac{\chi_0}{1+\xi^2[1+\gamma(q)]}\tanh\frac{\omega}{2T}\frac{1}{1+(\omega/\omega_s)^2}. \quad (42)$$

The q-dependent part has a peak at the AFM wave vector (π,π) with its intensity defined by the short-range AFM correlation length ξ (measured in lattice constant units). We take quite a small $\xi = 1-3$ to imitate incommensurate character of spin fluctuations with large correlation length $\xi \simeq 5$ observed at finite doping both in $La_{2-x}Sr_xCuO_4$ and $YBa_2Cu_3O_{7-x}$ in neutron scattering experiments.[47] For the frequency-dependent part we choose the scaling function with an enhanced intensity for frequencies $\omega < T$ and a large cutoff energy $\omega_s \simeq J$ according to neutron scattering experiments in single-layered cuprate $La_{2-x}Sr_xCuO_4$. It is important that the constant χ_0 in Eq. (42) which defines intensity of spin fluctuations at the AFM wave vector is normalized according to the following condition:

$$\frac{1}{N}\sum_i \langle \mathbf{S}_i \mathbf{S}_i\rangle = \frac{1}{N}\sum_q \chi_s(q)\int_{-\infty}^{+\infty}\frac{dz}{\exp(z/T)-1}\chi''_s(z) = \frac{\pi\omega_s}{2N}\sum_q \chi_s(q) = \frac{3}{4}n, \quad (43)$$

which gives

$$\chi_0 = \frac{3n}{2\pi\omega_s C_1}, \quad C_1 = \frac{1}{N}\sum_q \frac{1}{1+\xi^2[1+\gamma(q)]}.$$

In the approximation (41) we get for the interaction function (37)

$$\lambda_{11}(q,k-q|i\omega_\nu) = \lambda_{12}(q,k-q|i\omega_\nu) = -g^2(q,k-q)\chi_s(k-q)F_s(i\omega_\nu), \quad (44)$$

where

$$F_s(\omega_\nu) = \int_0^{\infty}\frac{2x\,dx}{x^2+(\omega_\nu/\omega_s)^2}\frac{1}{1+x^2}\tanh\frac{x}{2\tau} \quad (45)$$

is the spectral function, $\tau = T/\omega_s$.

Within the model (42) the static spin correlation functions (25) are calculated by using $\langle \mathbf{S}_q \mathbf{S}_{-q}\rangle = (\pi\omega_s/2)\chi_s(q)$. In Table I we give characteristic values for the static spin correlation functions and the constant χ_0 for different values of ξ.

TABLE I. Static spin correlations versus AFM correlation length ξ at different hole concentration δ.

ξ	δ	χ_0	χ_{1s}	χ_{2s}	$\chi_s(Q)/\chi_s(0)$
1	0.30	1.56	−0.072	0.019	3
3	0.10	7.40	−0.230	0.130	19
5	0.05	17.08	−0.311	0.213	51

To analyze a role of different interactions in the electron–spin-fluctuation scattering in Eq. (44) we consider the weak coupling approximation for the Eliashberg equation (33). It is given by the following approximation for the interaction (44):[48]

$$\lambda_{12}(q,k-q|i\omega_n - i\omega_m) \simeq -\lambda(q,k-q)\,\theta(\omega_s - |\omega_n|)\,\theta(\omega_s - |\omega_m|), \quad (46)$$

where we take $F_s(\omega_\nu) \simeq F_s(\omega_s) \simeq 1$ and introduce

$$\lambda(q,k-q)=g^2(q,k-q)\chi_s(k-q). \tag{47}$$

In the weak coupling limit we have for the anomalous GF

$$\tilde{G}^{\sigma}_{12}(k,i\omega_m)\simeq -\frac{\Phi^{\sigma}_k}{(\omega_m)^2+(\Omega^{\sigma}_k)^2}, \tag{48}$$

where $\Omega^2_k=[E^{\sigma}_k+\xi^{\sigma}_k(0)-\tilde{\mu}]^2+|\Phi^{\sigma}_k|^2$ is the QP energy in the superconducting state with the frequency-independent gap function Φ^{σ}_k. By performing summation over m for $\tilde{\Sigma}^{\sigma}_{12}(k,i\omega_n)$ in Eq. (36), we get the weak coupling BCS equation

$$\Phi^{\sigma}(k)=\frac{1}{N}\sum_q \{J(k-q)-\lambda(q,k-q)\}\frac{\Phi^{\sigma}_q}{2\Omega_q}\tanh\frac{\Omega_q}{2T}. \tag{49}$$

In comparison with the results of the diagram technique,[39] in Eq. (49) the kinematical interaction is also included in the effective coupling constant of the second order equation (47). Below we compare results for the superconducting T_c calculated in the weak coupling limit, Eq. (49), and those obtained from the Eliashberg equation (39).

The numerical calculations were performed using the fast Fourier transformation[49] for 32×32 cluster. In the summation over the Matsubara frequencies we used up to 700 points with the constant cutoff $\omega_{\max}=20t$. Usually 10–30 iterations were needed to obtain a solution for the self-energy with an accuracy of order 0.1%. The Padé approximation was used to calculate the one-electron spectral function $A_{11}(k,\omega)$ (29) and the density of states (DOS)

$$A(\omega)=\frac{1}{N}\sum_k A^{\sigma}_{11}(k,\omega) \tag{50}$$

on the real frequency axis.

The calculations were performed for several values of the t-J model parameters $(J/t,t'/t)$, the AFM correlation length ξ in the model function (42) with $\omega_s=J$, and the hole concentration $\delta=1-n$. Below we present results for $\delta=0.1-0.4$ and $\xi=1,3$ for the parameters $J=0.4,t'=0$ if other values are not indicated. All the energies and temperature are measured in units of t. To mimic suppression of AFM correlations with doping we usually take $\xi=3$ for $\delta=0.1$ and keep $\xi=1$ for $\delta=0.2-0.4$. Temperature effects are rather small for $T\leqslant0.1$ and therefore we present only results for $T=0.0125$.

A. Normal state

Results for the electron spectral density in the normal state, $A(k,\omega)=A_{11}(k,\omega)$ (29), are shown along the three symmetry directions in the BZ: $\Gamma(0,0)\rightarrow X(\pi,0)\rightarrow M(\pi,\pi)\rightarrow\Gamma$ in Fig. 1 for $\delta=0.1$, $\xi=1$, Fig. 2 for $\delta=0.1$, $\xi=3$, Fig. 3 for $\delta=0.1$, $\xi=1$, $t'=-0.3$, and Fig. 4 for $\delta=0.4$, $\xi=1$.

For small concentration of holes, $\delta=0.1$, we observe quite narrow QP peaks at the wave vectors crossing the Fermi surface (FS) along $M\rightarrow X$ and $M\rightarrow\Gamma$ directions. Along the $X\rightarrow\Gamma$ direction wave vectors are below the FS (see Fig. 9) and there are no QP peaks. In addition to the QP dispersion we see also a band of incoherent excitations with large dispersion below the Fermi energy $\omega<0$. The incoherent band is caused by the self-energy contribution peaked at the AFM wave vector (''shadow bands''). For $\xi=3$ in Fig. 2 the incoherent band has a higher intensity due to stronger spin-fluctuations weight at the AFM wave vector. An additional hopping between next neighbors changes the dispersion mostly at Γ and X points (see Fig. 3 with $t'=-0.3$) and increases the intensity of the incoherent band, especially at the X point (compare Figs. 1 and 3).

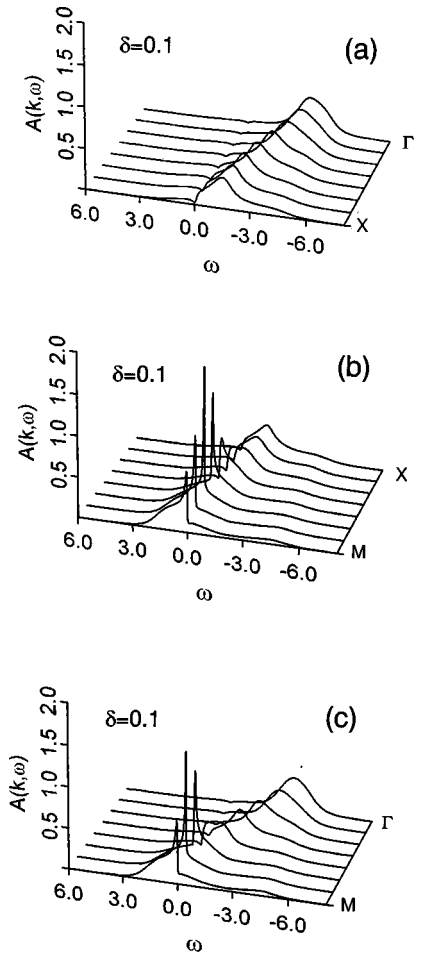

FIG. 1. Electron spectral density $A(k,\omega)$ for the hole concentration $\delta=0.1$ and AFM correlation length $\xi=1$.

With increasing hole concentration the dispersion of the QP band also increases and the intensity of QP peaks are enhanced as shown in Fig. 4 for $\delta=0.4$, $\xi=1$. At the same time the intensity of the incoherent excitations are suppressed: the ''high-energy feature'' below the Fermi energy at the X point for $\delta=0.1$, $\xi=3$ in Fig. 2 practically disappears for $\delta=0.4$, $\xi=1$ in Fig. 4. As was discussed by Shen and Schrieffer[50] (see also Ref. 51), the doping dependence of the spectral line shape near $(\pi,0)$ point can be explained by strong coupling of the QP hole excitations with collective excitations. In our model the latter are spin fluctuations which intensity at (π,π) point is proportional to ξ^2 [see Eq. (42)] resulting in strong suppression of the incoherent excitations with decreasing ξ and increasing δ. An important role of the next neighbor hopping t' in the explanation of the doping dependence of the spectral line shape near $(\pi,0)$ was also pointed out in Ref. 52.

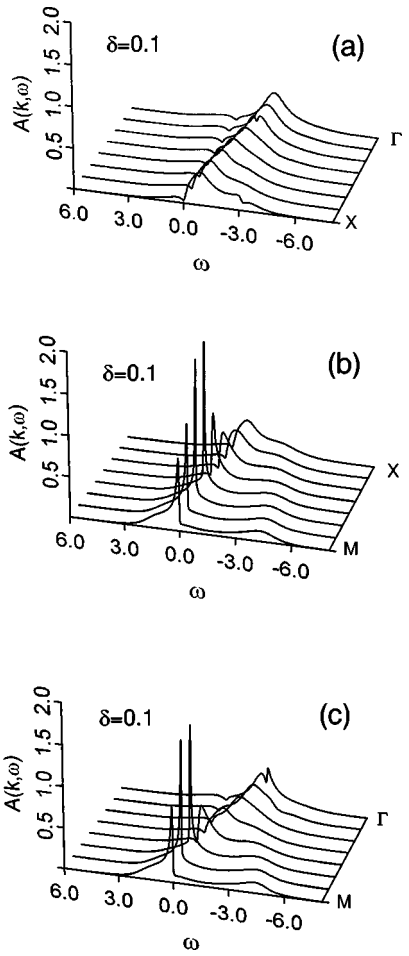

FIG. 2. Electron spectral density $A(k,\omega)$ for $\delta=0.1$ and $\xi=3$.

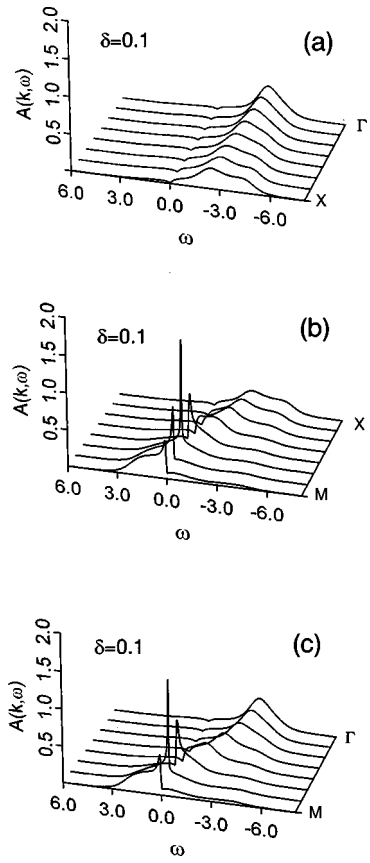

FIG. 3. Electron spectral density $A(k,\omega)$ for $\delta=0.1$, $\xi=1$, and next neighbor hopping parameter $t'=-0.3$.

These conclusions are supported by the doping dependence of the imaginary part of the self-energy $-\mathrm{Im}\,\Sigma(k,\omega)=-\mathrm{Im}\,\tilde{\Sigma}^{\sigma}_{11}(k,\omega+i\epsilon)$ shown in Fig. 5 for $\delta=0.1$, $\xi=3$ and Fig. 6 for $\delta=0.3$, $\xi=1$. With increasing hole concentration and decreasing AFM correlation length ξ the self-energy decreases due to suppression of electron scattering on spin-fluctuations. It is interesting to note that for the underdoped region, $\delta\leqslant 0.1$, $\mathrm{Im}\,\Sigma(k,\omega)$ for $T\leqslant\omega\leqslant J$ is approximately proportional to ω (see Fig. 5, especially the M point) while for the overdoped region, $\delta\geqslant 0.3$, for small ω we have $\mathrm{Im}\,\Sigma(k,\omega)\propto\omega^2$. However, our $(\mathbf{k},\omega)$ resolution is not high enough to prove a transition from the non-Fermi-liquid to the Fermi-liquid behavior with doping.

Our results for electron spectral functions are in a semiquantitative agreement with the numerical studies of the t-J model within the finite-temperature Lanczos method.[24] We observe also a large asymmetry between the photoemission ($\omega<0$) and the inverse photoemission ($\omega>0$) spectra. While the spectra below the FS in Figs. 1(a), 2(a), 3(a), 4(a) are strongly overdamped and show no QP peaks, the spectra for electrons outside the FS, e.g., at the $M(\pi,\pi)$ point in Figs. 1–3, show QP behavior. The main disagreement with the results of Ref. 24 is a smaller imaginary part of the self-energy, Figs. 5 and 6, which also results in a less pronounced incoherent part of the spectra below the FS. Partly this can be explained by the underestimation of the electron scattering on spin fluctuations. Namely, if we make an approximation $[1+\gamma(q)]\simeq|\mathbf{q}-\mathbf{Q}|^2$ in the spin susceptibility (42) which enhances the peak intensity at $Q=(\pi,\pi)$ we get much stronger scattering and a more intensive incoherent band. To enhance the incoherent contribution and to fulfill the Luttinger theorem it was proposed in Ref. 44 to add to the self-energy (27) a momentum-independent part $\mathrm{Im}\,\Sigma(\omega)=-c\omega^2$, with quite a large value at maximum $\simeq 3.5t$. However, this fitting is difficult to justify. We find also a reasonable agreement of our results for the spectral function for $\delta=0.1$, $\xi=3$, including both the coherent QP dispersion and incoherent band, with the calculations in Ref. 23 done by the exact-diagonalization technique for a finite cluster of 20 lattice sites with 2 holes ($\delta=0.1$).

In Fig. 7 we show the QP dispersion $E(\mathbf{k})$ for $\delta=0.1$, $\xi=3$ and $t'=0$, ± 0.1 (upper panel) and $\delta=0.1$, $\xi=3$ and $\delta=0.4$, $\xi=1$ (lower panel) which are calculated from the maxima of spectral density. As we see, the QP band width strongly increases with doping while the next neighbor hopping t' change the dispersion mostly at $\Gamma(0,0)$ and $X(\pi,0)$ points. These results can be already explained within the spectrum E_k in MFA, Eq. (20). Written in the form

$$E^{\sigma}_k=-4t\gamma(k)Q[1+\chi_{1s}/Q^2]-4t'\gamma'(k)Q[1+\chi_{2s}/Q^2]$$
$$=-t_{\mathrm{eff}}\gamma(k)-t'_{\mathrm{eff}}\gamma'(k),$$

it shows a strong dependence of the effective hopping parameters on the static AFM correlation functions (25): $\chi_{1s}=\langle\mathbf{S}_i\mathbf{S}_{i+a_1}\rangle$, $\chi_{2s}=\langle\mathbf{S}_i\mathbf{S}_{i+a_2}\rangle$. For small hole concentration and large AFM correlation length, e.g., $\delta=0.1$, $\xi=3$, we

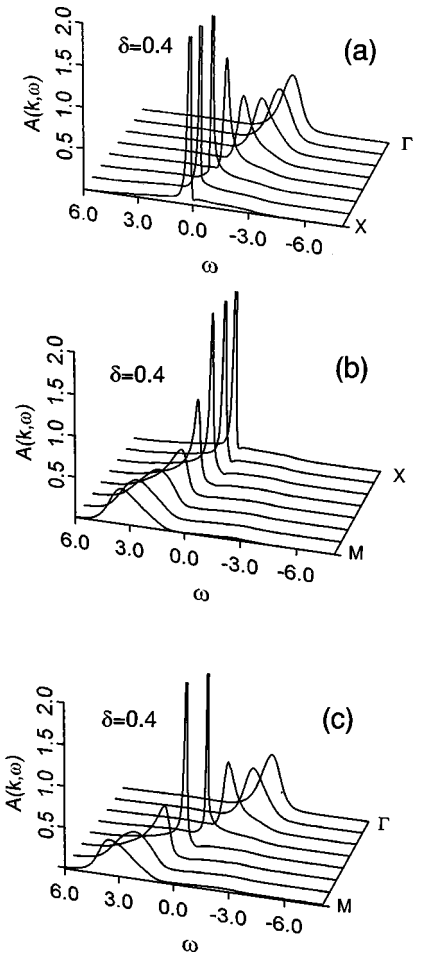

FIG. 4. Electron spectral density $A(k,\omega)$ for $\delta=0.4$ and $\xi=1$.

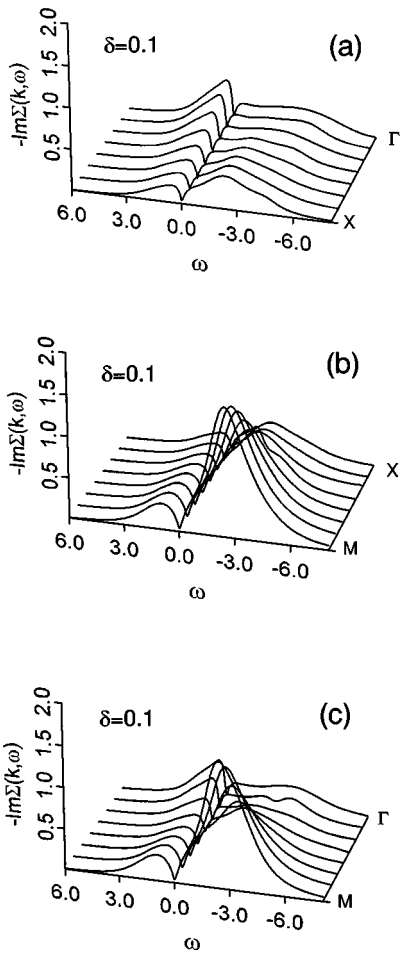

FIG. 5. Imaginary part of the electron self-energy $-\mathrm{Im}\,\tilde{\Sigma}^{\sigma}_{11}(k,\omega+i\epsilon)$ for $\delta=0.1$ and $\xi=3$.

have $\chi_{1s}=-0.23$, $\chi_{2s}=0.13$ (see Table I) and $t_{\mathrm{eff}}\simeq 0.53t$, $t'_{\mathrm{eff}}\simeq 1.25t'$. At large hole concentration, e.g., $\delta=0.4$, $\xi=1$, we have $\chi_{1s}=-0.06$, $\chi_{2s}=0.016$ and $t_{\mathrm{eff}}\simeq 2.5t$, $t'_{\mathrm{eff}}\simeq 2.7t'$. The self-energy additionally renormalizes the spectrum but the general δ,ξ dependence obtained in the MFA agrees quite well with that observed in Fig. 7.

Here we would like to point out that in the large-N expansion technique, both for the slave boson[29,30] and the Baym-Kadanoff variational GF,[32,33] the narrowing of the band due to the discussed above AFM correlations is ignored. In the $1/N$ expansion the static spin correlation functions χ_{1s},χ_{1s} appear to be of the higher order in $1/N$ and therefore are omitted. Moreover, the factor Q in the spectrum in the MFA, Eq. (20) is also underestimated. We have in Eq. (20) $Q_{\sigma}=\langle X_i^{00}+X_i^{\sigma\sigma}\rangle=(1+\delta)/2$ while in the $1/N$ expansion $Q=\langle X_i^{00}\rangle=\delta$ since the correlation function $\langle X_i^{\sigma\sigma}\rangle$ is of the order $1/N$ and is disregarded. These underestimations of the strong kinematical interaction in the large-N expansion change the doping dependence of the QP spectrum in MFA in comparison with the real situation $N=2$.

Figure 8 shows the density of states $A(\omega)$ for $\delta=0.1$, $\xi=3$ (dashed line) and $\delta=0.4$, $\xi=1$ (solid line). Since the incoherent band is strongly suppressed at large hole concentration ($\delta=0.4$) and small AFM correlation length ($\xi=1$), the DOS has a nearly symmetric form with a broad band width (of the order of $7t$) in comparison with the highly asymmetric one for low doping ($\delta=0.1$) where the high density of states below the Fermi level is due to the incoherent band. In that respect the DOS at $\delta=0.1$ agrees quite well with the results of numerical studies by the finite-temperature Lanczos method[24] where the single-particle DOS is also quite asymmetric with large incoherent part below the FS. Moreover, the absolute values of the DOS at maximum are close to each other [in Ref. 24, DOS $N(\omega)=(1+\delta)A(\omega)$ where $A(\omega)$ is given by Eq. (50)].

Now we consider the results for the electron occupation numbers (24) $n_{\mathbf{k},\sigma}=\langle X_k^{\sigma 0}X_k^{0\sigma}\rangle=[(1+\delta)/2]N_{\mathbf{k}\sigma}$. In Fig. 9 the function $N(\mathbf{k})=N_{\mathbf{k}\sigma}$ is shown for different hole concentrations: (a) $\delta=0.1$, $\xi=3$, and (b)–(d) $\delta=0.2-0.4$, $\xi=1$. The shape of the FS changes from holelike around the $M(\pi,\pi)$ point of BZ at small doping to electronlike around the $\Gamma(0,0)$ point of BZ for large doping. We obtain quite a small drop of $N(\mathbf{k})$ at the FS especially at small doping, which is a specific feature of strongly correlated electronic systems. Large occupation numbers throughout the BZ are due to the incoherent contribution in the spectral density $A(k,\omega)$ under the Fermi level (see Figs. 1–4). The evolution of the FS with hole concentration is also shown in Fig. 10 by bold solid lines. The maximal occupation numbers for electrons $n_{\mathbf{k},\sigma}=(1+\delta)N(\mathbf{k})/2\leqslant 0.55$ for $\delta=0.1$ agrees with the results of the exact-diagonalization technique for finite clusters.[23] According to Eq. (40), we also have inequality n

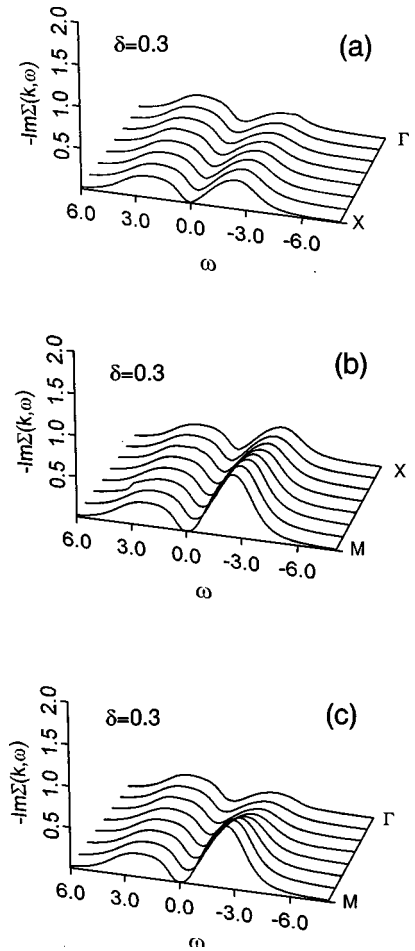

FIG. 6. Imaginary part of the electron self-energy $-\mathrm{Im}\,\tilde{\Sigma}^{\sigma}_{11}(k,\omega+i\epsilon)$ for $\delta=0.3$ and $\xi=1$.

$\leqslant 1$ that results from the restriction of no double occupancy of lattice sites in the t-J model.

Concerning the volume of the electron FS, it appears to be proportional at small doping to $(1-\delta)$, e.g., for $\delta=0.1$, 0.2 the ratio of the BZ part for $k<k_F$ to the whole BZ are close to 90 and 80 %, respectively, while according to

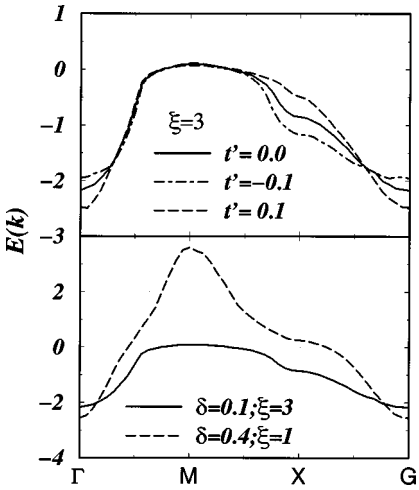

FIG. 7. Electron quasiparticle spectrum $E(\mathbf{k})$ for $\delta=0.1$ and $t'=0$, ± 0.1, $\xi=3$ (upper panel), and $\delta=0.1$, $\xi=3$ (solid line) and $\delta=0.4$, $\xi=1$ (dashed line) (lower panel).

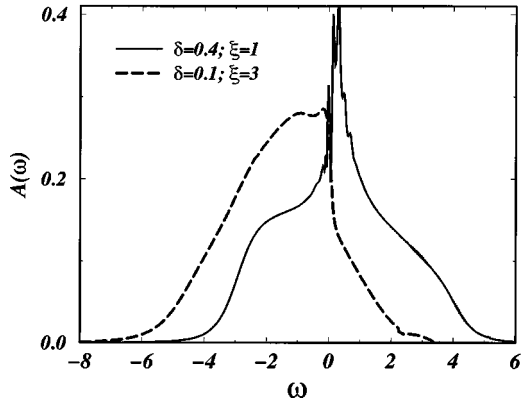

FIG. 8. Electron density of states $A(\omega)$ for $\delta=0.1$, $\xi=3$ (dashed line) and $\delta=0.4$, $\xi=1$ (solid line).

the Luttinger theorem the ratio should be equal to $(1-\delta)/2$. It is possible to obtain a large FS at small doping if one introduces a strong incoherent part in the DOS below the FS as it has been proposed in Ref. 44. However, the one (sub)band t-J model could violate the Luttinger theorem since it is derived for the Mott-Hubbard insulating state which may not have an adiabatic connection to a noninteracting electron gas. A violation of the Luttinger theorem in the high-temperature series for the momentum distribution function of the two-dimensional t-J has been recently reported in Ref. 53. Our results for the FS at $\delta=0.2$, see Figs. 9(b) and 10(b), are in quantitative agreement with that one presented in Ref. 53 concerning both the shape of the FS [hole pockets at $(\pm\pi,\pm\pi)$ points—see dotted line in Fig. 5 of Ref. 53] and the volume of the FS: it is equal to 0.8 instead of 0.4 according to the Luttinger theorem. In our calculations we have also observed quite a strong dependence of the FS shape on the next-nearest hopping parameter t' and the AFM correlation length ξ. In any case, to study

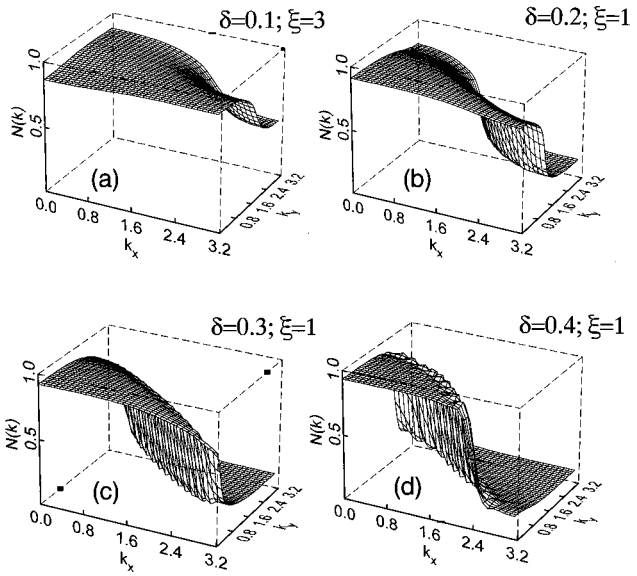

FIG. 9. Electron occupation numbers $N(\mathbf{k})$ $[n_{k,\sigma}=(1+\delta)N(\mathbf{k})/2]$ versus $\mathbf{k}$ $(0\leqslant k_x,k_y\leqslant\pi)$ for different hole concentration δ and AFM correlation length ξ: $\delta=0.1$, $\xi=3$ (a), $\delta=0.2$, $\xi=1$ (b), $\delta=0.3$, $\xi=1$ (c), $\delta=0.4$, $\xi=1$ (d).

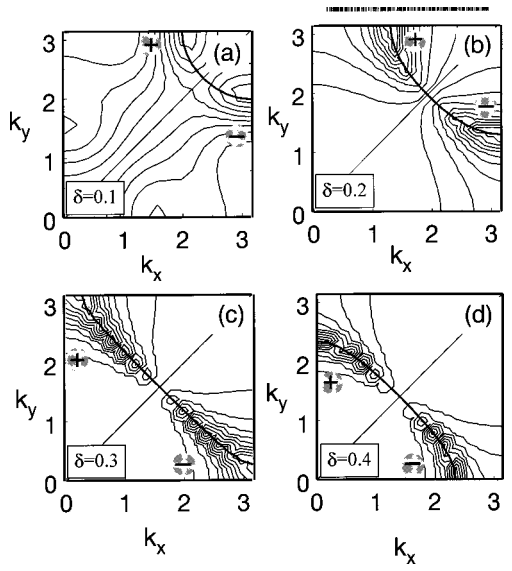

FIG. 10. The Fermi surface (bold solid lines) and the gap function $\Phi(\mathbf{k},0)$ [thin solid lines with $(+)$ and $(-)$ showing the sign of the gap] versus $\mathbf{k}$ $(0\leqslant k_x,k_y\leqslant\pi)$ for different hole concentration δ and AFM correlation length ξ: $\delta=0.1$, $\xi=3$ (a), $\delta=0.2$, $\xi=1$ (b), $\delta=0.3$, $\xi=1$ (c), $\delta=0.4$, $\xi=1$ (d).

the FS in strongly correlated systems one should consider the original Hubbard model with upper and lower subbands since a weight transfer between the subbands with doping away from the half-filled insulating state could drastically change the shape of the FS.

B. Superconducting state

The results of the numerical solution of the linearized Eliashberg equation (39) are presented in Figs. 10–13. Figure 10 shows the contour plots in a quarter of BZ $(0\leqslant k_x,k_y\leqslant\pi)$ for the static gap function $\Phi(k)=\Phi(k,\omega=0)$. At a small doping, $\delta=0.1$ [Fig. 10(a)], it has a more complicated k dependence, with two positive and two negative maxima [shown by $(+)$ and $(-)$] while at $\delta\geqslant 0.2$ only one positive and one negative maximum survive [Figs. 10(b)–10(d)]. This is shown in Fig. 11 for $\Phi(k)$ in $\mathbf{k}$ space for a small concentration of holes, $\delta=0.1$ (a), and for a nearly optimal one, $\delta=0.3$ (b). The $\Phi(\mathbf{k})$ dependence has a complicated form that cannot be described by the simple $(\cos k_x-\cos k_y)$ function usually used for d-wave symmetry. However, in all cases the gap function obeys B_{1g} symmetry: $\Phi(k_x,k_y)=-\Phi(k_y,k_x)$ which breaks the fourfold symmetry of the FS in $\mathbf{k}$ space.

The frequency dependence of the gap function $\Phi(k,\omega)$ is also anomalous. In Fig. 12 we show the ω dependence for the real $\mathrm{Re}\,\Phi(k,\omega)$ and imaginary $\mathrm{Im}\,\Phi(k,\omega+i\epsilon)$ parts of the gap function for $\delta=0.3$, $\xi=1$ at the $X(0,\pi)$ point of the BZ.

In Fig. 13 we present the superconducting T_c versus hole concentration δ for AFM correlation length $\xi=1$ (solid line) and $\xi=3$ (dashed line), obtained from numerical solution of Eq. (39). With increasing AFM correlation length ξ effective electron-electron coupling $\lambda_{12}(q,k-q|i\omega_\nu)$ mediated by spin fluctuations $\chi_s(k-q)$ also increases, which raises T_c. For comparison in Fig. 14 we also present superconducting

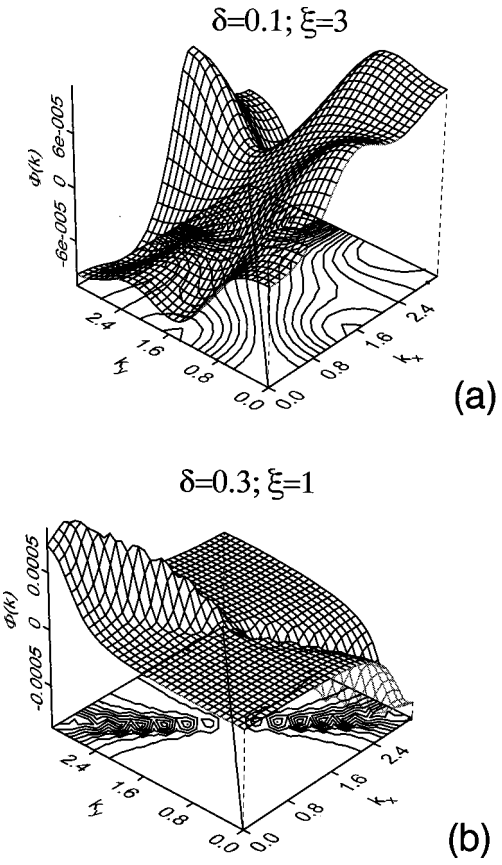

FIG. 11. The gap function $\Phi(\mathbf{k},\omega=0)$ versus $\mathbf{k}$ for $\delta=0.1$, $\xi=3$ (a), $\delta=0.3$, $\xi=1$ (b).

temperature T_c versus hole concentration δ for AFM correlation length $\xi=1$ in the weak coupling approximation, Eq. (49), for the full vertex $J(k-q)-\lambda(q,k-q)$ (solid line), the vertex with $t(q)=0$ in $\lambda(q,k-q)$ (dashed line), and in the MFA with $\lambda(q,k-q)=0$ (dotted line). We see that in the weak coupling approximation T_c is much higher in comparison with that one obtained from the frequency-dependent equation (39) for the same static susceptibility, i.e., $\xi=1$ in Eq. (42). The most important contribution in the weak coupling approximation comes from MFA, i.e., $J(k-q)$ in Eq. (49). The second order contribution $\lambda(q,k-q)$

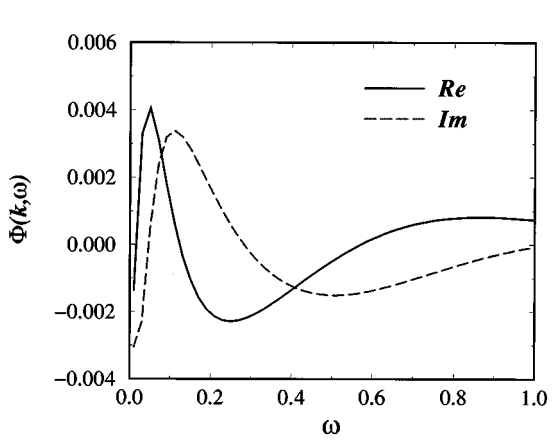

FIG. 12. Real $\mathrm{Re}\,\Phi(k,\omega)$ and imaginary $\mathrm{Im}\,\Phi(k,\omega+i\epsilon)$ parts of the gap function versus ω for $\delta=0.3$, $\xi=1$ at $(k_x,k_y)=(0,\pi)$.

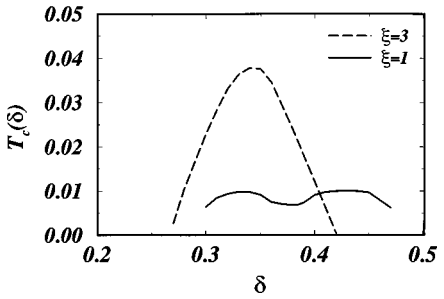

FIG. 13. The superconducting temperature T_c versus hole concentration δ for AFM correlation length $\xi=1$ (solid line) and $\xi=3$ (dashed line), obtained from Eq. (39).

$=g^2(q,k-q)\chi_s(k-q)$ enhances T_c both due to kinematical $t(q)$ and exchange $J(k-q)$ interactions. For a larger AFM correlation length superconducting T_c is greatly enhanced in the weak coupling approximation, e.g., $T_c \simeq 0.1$ for $\xi=3$.

To elucidate the role of AFM short-range fluctuations in the model and, in particular, the strong dependence of T_c on the AFM correlation length ξ we present in Table I the ξ dependence of the static correlation functions χ_{1s}, χ_{2s} and the constant χ_0 in Eq. (42). The latter, as well the ratio $\chi_s(Q)/\chi_s(q=0)$, estimates the electron-spin fluctuation coupling while the static correlation functions χ_{1s}, χ_{2s}, Eq. (25), define the bandwidth in the MFA, Eq. (20) as discussed above. The large increase of these parameters seen in Table I, with increasing ξ from their values at $\xi=1$, explains changes in the spectral functions $A(k,\omega)$ and strong T_c enhancement.

At the same time the peak position of $T_c(\delta)$ around the hole concentration $\delta \simeq 0.33$ does not change much with ξ. As Fig. 10 shows, at this concentration the FS crosses the $(\pm\pi,0),(0,\pm\pi)$ points of the BZ. Since the pairing interaction Eq. (44) is proportional to the spin susceptibility $\chi_s(k-q)$ with the maximal contribution at $\mathbf{k}-\mathbf{q}=Q$ the strongest pairing occurs for electrons at the FS with $k=(\pm\pi,0),(0,\pm\pi)$ coupled by the AFM wave vector $Q=(\pi,\pi)$. This scenario is characteristic for spin-fluctuation pairing[9] and has been discussed recently by Shen and Schrieffer[50] in connection with the anomalous momentum and temperature dependence of the spectral line shape in ARPES experiments. Experimentally the highest T_c is observed at the optimal doping of $\delta \simeq 0.16$. To obtain maximal T_c in our calculations at the lower hole concentration the FS should be large and run along the diagonals $(\pm\pi,0)-(0,\pm\pi)$ at this hole concentration. In the spin-polaron t-J model[20] the $T_c(\delta)$ curve has a narrow peak at the optimal doping $\delta=0.15-0.25$, depending on the next neighbor hopping $t'=\pm 0.1t$, since in that case the FS is close to the AFM BZ along the diagonals $(\pm\pi,0)-(0,\pm\pi)$ already at a low concentration of doped holes.

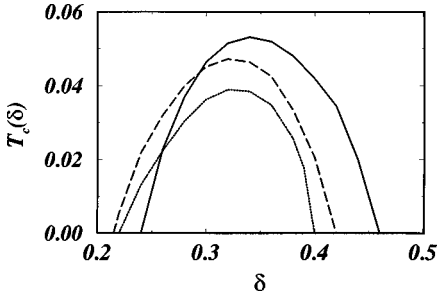

FIG. 14. The superconducting temperature T_c versus hole concentration δ for AFM correlation length $\xi=1$ in the weak coupling approximation Eq. (49) for the full vertex (solid line), the vertex with $t(q)=0$ (dashed line), and in the MFA with $\lambda(q,k-q)=0$ (dotted line).

V. CONCLUSIONS

In the present paper a theory of electron spectrum and superconducting pairing in the t-J model (4) in a paramagnetic state was developed by employing the projection technique[40] for the two-time GF (Ref. 41) in terms of Hubbard operators. The obtained self-consistent system of Eliashberg equations for the matrix GF (33) and the self-energy (27) in comparison with the diagram technique[39] has an additional contribution proportional to the second order of the kinematical interaction $t(q)$ which gives an important contribution in comparison to the exchange interaction $J(k-q)/2$ in the vertex (23).

The one-electron spectral functions, the superconducting T_c, and the gap function were calculated by a numerical solution of the linearized system of Eliashberg equations (38),(39). To describe kinematical and exchange interactions of electrons with spin fluctuations a model dynamic spin susceptibility (42) with short-range AFM correlation length ξ was used.

The results for the electron spectral density (see Figs. 1–4) show QP excitations at the FS crossing and a dispersive incoherent band. For small hole concentration and large AFM correlation length ξ the QP dispersion is small while the intensity of the incoherent band is quite large. With doping the QP bandwidth strongly increases and the incoherent band is suppressed. Our results for electron spectral functions are in semiquantitative agreement with the numerical studies of the t-J model within the finite-temperature Lanczos method[24] and also agree quite well with the studies by the exact-diagonalization technique.[23] To perform a quantitative comparison of our numerical results with ARPES investigations[3] one has to consider a more general t-t'-t''-J model with the three-site terms as has been discussed recently (see, e.g., Ref. 54).

The occupation numbers $N(\mathbf{k})$ have the characteristic behavior for strongly correlated systems, Fig. 9. Being large throughout the BZ they show only a small drop at the FS. The volume of the FS at small doping is proportional to the hole concentration δ, as shown in Fig. 10, which violates the Luttinger theorem. However, our result for the volume of the FS for $n=0.8$ is in quantitative agreement with the recent numerical results of Putikka *et al.*[53]

The superconducting pairing due to the exchange and the kinematic interactions (in second order) has d-wave symmetry, Fig. 11, and high T_c, Fig. 13. In the weak coupling approximation, Eq. (49), a much larger T_c is observed, Fig. 14. Our calculations confirm the results of the d-wave superconducting pairing obtained within the spin-polaron t-J model.[20] One can argue that our result for the d-wave superconducting pairing for the 2D t-J model contradicts the con-

clusions of Ref. 26 based on numerical results for finite clusters. Moreover, it can be rigorously proved (see, e.g., Ref. 55) that there is no long-range superconducting order in two-dimensional systems due to phase fluctuations of the order parameter. However, we consider Eliashberg equations which are really based on the mean field approximation—the phase of the order parameter is fixed in Eq. (38) by taking it to be real. Therefore the superconducting T_c in our calculations is the temperature of the Cooper pair formation while the temperature of phase coherence should be calculated by taking into account the coupling between the CuO_2 planes. In our calculations within the Eliashberg theory for the 2D t-J model we observe Cooper pair formation but in a restricted region of hole doping. More detailed numerical studies are needed, including investigation of the spin(charge) gap formation for the more general t-t'-J model to verify the scenario of Cooper pair formation in the highly underdoped region.

The important advantage of the proposed microscopical theory for the d-wave spin-fluctuation superconducting pairing, in comparison with phenomenological approaches based on Fermi-liquid models close to AFM instability, is that we have used only two basic parameters of the model, the hopping energy t and the (super)exchange energy J which are characteristic in strongly correlated systems.[27] We have no additional fitting parameters for the electron–spin-fluctuation interaction since the electron scattering on spin-charge fluctuations is a result of the kinematical and exchange interactions. Some uncertainty in the interaction is due to the noncrossing approximation (26) where vertex corrections, as in the diagram technique in Ref. 39, are neglected. We think that vertex corrections should not change the main conclusions of our calculations. At least, we can argue that in our approach, where the model spin susceptibility (42) with small AFM correlation length $\xi=1-3$ is used, the vertex renormalization, estimated as $\chi_s(Q)/\chi_s(0)$ (see Ref. 56), should not be large (see Table I). More detailed studies within the developed theory are planned to elucidate some of the unresolved problems of the present investigation.

ACKNOWLEDGMENTS

We gratefully acknowledge stimulating discussions with P. Horsch, R. Zeyher, and A. Liechtenstein. We are also indebted to G. Jackeli and V. Yushankhai for valuable discussions and remarks. One of the authors (N.P.) thanks Professor P. Fulde for the hospitality extended to him during his stay at the MPIPKS where a major part of this work was done. We acknowledge usage of computational facilities of the Max-Planck-Institute in Stuttgart kindly provided to us by Professor L. Hedin. Partial financial support by the INTAS-RFBR Program, Grant No. 95–591 and by NREL, Subcontract No. AAX-6-16763-01 is acknowledged.

[1] P. W. Anderson, Science **235**, 1196 (1987).
[2] P. W. Anderson, *The Theory of Superconductivity in the High-T_c Cuprates* (Princeton University Press, Princeton, NJ, 1997).
[3] Z.-X. Shen and D. S. Dessau, Phys. Rep. **253**, 1 (1995).
[4] H. Ding, T. Yokota, J. C. Campuzano, T. Takahashi, M. R. Norman, T. Mochiku, K. Kadowaki, and J. Giapintzakis, Nature (London) **382**, 51 (1996).
[5] A. G. Loeser, Z.-X. Shen, D. S. Dessau, D. S. Marshall, C. H. Park, P. Fournier, and A. Kapitulnik, Science **273**, 325 (1996).
[6] M. R. Norman, H. Ding, M. Randeria, J. C. Campuzano, T. Yokoya, T. Takeuchi, T. Takahashi, T. Mochiku, K. Kadowaki, P. Guptasarma, and D. G. Hinks, Nature (London) **392**, 157 (1998).
[7] Ch. Renner, B. Revaz, J.-Y. Genoud, K. Kadowaki, and Ø. Fisher, Phys. Rev. Lett. **80**, 149 (1998); Ch. Renner, B. Revaz, K. Kadowaki, I. Maggio-Aprile, and Ø. Fisher, *ibid.* **80**, 3660 (1998).
[8] N. Miyakawa, P. Guptasarma, J. F. Zasadzinski, D. G. Hinks, and K. E. Gray, Phys. Rev. Lett. **80**, 157 (1998).
[9] D. J. Scalapino, Phys. Rep. **250**, 329 (1995).
[10] F. C. Zhang and T. M. Rice, Phys. Rev. B **37**, 3759 (1988).
[11] S. Schmitt-Rink, C. M. Varma, and A. E. Ruckenstein, Phys. Rev. Lett. **60**, 2793 (1988).
[12] C. L. Kane, P. A. Lee, and N. Read, Phys. Rev. B **39**, 6880 (1989).
[13] G. Martinez and P. Horsch, Phys. Rev. B **44**, 317 (1991).
[14] Z. Liu and E. Manousakis, Phys. Rev. B **45**, 2425 (1992).
[15] A. Scherman and M. Schreiber, Phys. Rev. B **48**, 7492 (1993); **50**, 12 887 (1994).
[16] N. M. Plakida, V. S. Oudovenko, and V. Yu. Yushankhai, Phys. Rev. B **50**, 6431 (1994).
[17] B. O. Wells, Z.-X. Shen, A. Matsuura, D. M. King, M. A. Kastner, M. Greven, and R. J. Birgeneau, Phys. Rev. Lett. **74**, 964 (1995).
[18] E. Dagotto, A. Nazarenko, and A. Moreo, Phys. Rev. Lett. **74**, 310 (1995).
[19] V. I. Belinicher, A. L. Chernyshev, A. V. Dotsenko, and O. P. Sushkov, Phys. Rev. B **51**, 6076 (1995).
[20] N. M. Plakida, V. S. Oudovenko, P. Horsch, and A. I. Liechtenstein, Phys. Rev. B **55**, R11997 (1997).
[21] A. Scherman and M. Schreiber, Phys. Rev. B **52**, 10 621 (1995).
[22] E. Dagotto, Rev. Mod. Phys. **66**, 763 (1994).
[23] W. Stephan and P. Horsch, Phys. Rev. Lett. **66**, 2258 (1991).
[24] J. Jaklič and P. Prelovśek, Phys. Rev. B **55**, R7307 (1997).
[25] Shiwei Zhang, J. Carlson, and J. E. Gubernatis, Phys. Rev. Lett. **78**, 4486 (1997).
[26] C. T. Shih, Y. C. Chen, H. Q. Lin, and T. K. Lee, Phys. Rev. Lett. **81**, 1294 (1998).
[27] P. W. Anderson, Adv. Phys. **46**, 3 (1997).
[28] Y. Suzumura, Y. Hasegawa, and H. Fukuyama, J. Phys. Soc. Jpn. **57**, 401 (1988).
[29] G. Kotliar and J. Liu, Phys. Rev. Lett. **61**, 1784 (1988).
[30] M. Grilli and G. Kotliar, Phys. Rev. Lett. **64**, 1170 (1990).
[31] E. Arrigoni, C. Castellani, M. Grilli, R. Raimondi, and G. C. Strinati, Phys. Rep. **241**, 291 (1994).
[32] A. Greco and R. Zeyher, Europhys. Lett. **35**, 115 (1996).
[33] R. Zehher and A. Greco, Z. Phys. B **104**, 737 (1997); (unpublished).
[34] R. O. Zaitsev, Sov. Phys. JETP **43**, 574 (1976).

[35] Yu. A. Izyumov and Yu. N. Scryabin, *Statistical Mechanics of Magnetically Ordered Systems* (Consultant Bureau, New York, 1989).
[36] R. O. Zaitsev and V. A. Ivanov, Fiz. Tverd. Tela (Leningrad) **29**, 2554 (1987); **29**, 3111 (1987); Int. J. Mod. Phys. B **5**, 153 (1988); Physica C **153-155**, 1295 (1988).
[37] N. M. Plakida, V. Yu. Yushankhai, and I. V. Stasyuk, Physica C **160**, 80 (1989).
[38] V. Yu. Yushankhai, N. M. Plakida, and P. Kalinay, Physica C **174**, 401 (1991).
[39] Yu. A. Izyumov and B. M. Letfulov, J. Phys.: Condens. Matter **3**, 5373 (1991).
[40] N. M. Plakida, Phys. Lett. **43A**, 481 (1973).
[41] D. N. Zubarev, Sov. Phys. Usp. **3**, 320 (1960).
[42] J. Hubbard, Proc. R. Soc. London, Ser. A **285**, 542 (1965).
[43] L. F. Feiner, J. H. Jefferson, and R. Raimondi, Phys. Rev. B **53**, 8751 (1996).
[44] P. Prelovšek, Z. Phys. B **103**, 363 (1997).
[45] G. Jackeli and N. M. Plakida, Theor. Math. Phys. **114**, 426 (1998).
[46] J. Jaklič, and P. Prelovšek, Phys. Rev. Lett. **74**, 3411 (1995); **75**, 1340 (1995).
[47] K. Yamada, C. H. Lee, K. Kurahashi, J. Wada, S. Wakimoto, S. Ueki, H. Kamura, and Y. Endoh, Phys. Rev. B **57**, 6165 (1998); H. A. Mook, Pengcheng Dai, S. M. Hayden, G. Aeppli, T. G. Perring, and F. Dogan, Nature (London) **395**, 580 (1998).
[48] Ph. Allen and B. Mitrović, Solid State Phys. **37**, 1 (1982).
[49] J. W. Serene and D. W. Hess, Phys. Rev. B **44**, 3391 (1991).
[50] Z.-X. Shen and J. R. Schrieffer, Phys. Rev. Lett. **78**, 1771 (1997).
[51] J. Schmalian, D. Pines, and B. Stojković, Phys. Rev. Lett. **80**, 3839 (1998).
[52] C. Kim, P. J. White, and Z.-X. Shen *et al.*, Phys. Rev. Lett. **80**, 4245 (1998).
[53] W. O. Putikka, M. U. Luchini, and R. R. P. Singh, Phys. Rev. Lett. **81**, 2966 (1998).
[54] V. Yu. Yushankhai, V. S. Oudovenko, and R. Hayn, Phys. Rev. B **55**, 15 562 (1997).
[55] G. Su and M. Suzuki, Phys. Rev. B **58**, 117 (1998).
[56] J. R. Schrieffer, J. Low Temp. Phys. **99**, 397 (1995).